

## Supramolecular chemistry and crystal engineering\*

ASHWINI NANGIA

School of Chemistry, University of Hyderabad, Prof. C.R. Rao Road, Gachibowli, Central University PO, Hyderabad 500 046

e-mail: ashwini.nangia@gmail.com

**Abstract.** Advances in supramolecular chemistry and crystal engineering reported from India within the last decade are highlighted in the categories of new intermolecular interactions, designed supramolecular architectures, network structures, multi-component host–guest systems, cocrystals, and polymorphs. Understanding self-assembly and crystallization through X-ray crystal structures is illustrated by two important prototypes – the large unit cell of elusive saccharin hydrate,  $\text{Na}_{16}(\text{sac})_{16} \cdot 30\text{H}_2\text{O}$ , which contains regular and irregular domains in the same structure, and by the Aufbau build up of zinc phosphate framework structures, e.g. ladder motif in  $[\text{C}_3\text{N}_2\text{H}_{12}][\text{Zn}(\text{HPO}_4)_2]$  to layer structure in  $[\text{C}_3\text{N}_2\text{H}_{12}][\text{Zn}_2(\text{HPO}_4)_3]$  upon prolonged hydrothermal conditions. The pivotal role of accurate X-ray diffraction in supramolecular and structural studies is evident in many examples. Application of the bottom-up approach to make powerful NLO and magnetic materials, design of efficient organogelators, and crystallization of novel pharmaceutical polymorphs and cocrystals show possible future directions for interdisciplinary research in chemistry with materials and pharmaceutical scientists. This article traces the evolution of supramolecular chemistry and crystal engineering starting from the early nineties and projects a center stage for chemistry in the natural sciences.

**Keywords.** Crystallization; hydrogen bond; materials; nanoscience; pharmaceutical; self-assembly.

### 1. Introduction

The award of Nobel Prize to Charles J Pedersen, Donald J Cram and Jean-Marie Lehn in 1987 marked the emergence of a new branch of chemistry, namely supramolecular chemistry. Lehn defined supramolecular chemistry as ‘chemistry beyond the molecule’, i.e. the chemistry of molecular aggregates assembled via non-covalent interactions.<sup>1,2</sup> Two decades later, supramolecular chemistry<sup>3,4</sup> is an important, interdisciplinary branch of science encompassing ideas of physical and biological processes. The roots of this interdisciplinary science lie in more than one field. Host–guest chemistry goes back to the discovery of chlorine hydrate by Humphrey Davy in 1810 and Wöhler’s  $\text{H}_2\text{S}$  clathrate of  $\beta$ -quinol in 1849. Supramolecular chemistry in biological processes is nothing but molecular binding recognized by Paul Ehrlich (1906) and Emil Fischer’s lock-and-key principle (1894) brought in complementarity and selectivity. Molecular recognition at the supramolecular level is mediated by com-

plementarity – even for like molecules it is the dissimilar portions of functional groups that interact with one another. An electropositive hydrogen bond donor approaches an electronegative acceptor ( $D^{\delta-} \cdots H^{\delta+} \cdots A^{\delta-}$ ), cation–anion electrostatic interaction in salts and metal complexes ( $M^+X^-$ ), and bumps in one part of the molecule fit into hollows of another portion (hydrophobic interactions), and so on. Even as the fundamental recognition processes that guide supramolecular aggregation are governed by the same principles and forces, the chemical systems studied are broadly classified into two major categories (figure 1): molecular recognition in solution is generally referred to as supramolecular chemistry, and organized self-assembly in the solid state as crystal engineering.<sup>5,6</sup> There have been significant advances in both these streams over the last two decades, and this review presents some salient developments and highlights.

### 2. Research overview

#### 2.1 Intermolecular interactions

Systematic studies on the nature of hydrogen bonds and intermolecular interactions lie at the heart of

\*Reproduced from ‘Current Trends in Science’ Platinum Jubilee Special Publication, Indian Academy of Sciences, Bangalore, 2009, pp. 35–51 with minor editorial changes

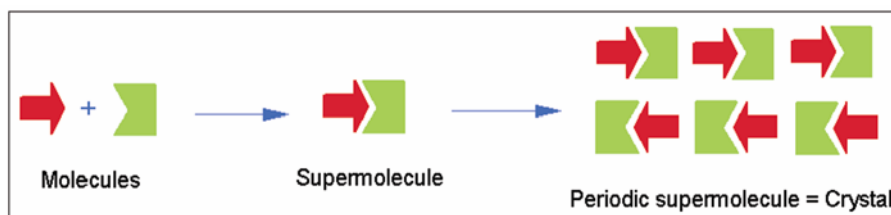


**Figure 1.** Molecular recognition of molecules to give supermolecule and periodic arrangement of supermolecules in a crystal lattice. Note the complementary shape and bonding feature of interacting molecules.

**Table 1.** Strength scale of different intermolecular interactions and hydrogen bonds.

Interaction type	Energy (kcal mol <sup>-1</sup> )	Examples
Very strong H bonds	15–40	O–H...O <sup>-</sup> , F–H...F <sup>-</sup>
Coordinative bonds	20–45	M–N, M–O
Strong hydrogen bonds	5–15	O–H...O, N–H...O
Weak hydrogen bonds	1–4	C–H...O, O–H... $\pi$
van der Waals interactions	0.5–2	CH <sub>3</sub> ...CH <sub>3</sub> , CH <sub>3</sub> ...Ph
Heteroatom interactions	1–2	N...Cl, I...I, Br...Br
$\pi$ -stacking	2–10	Ph...Ph, nucleobases

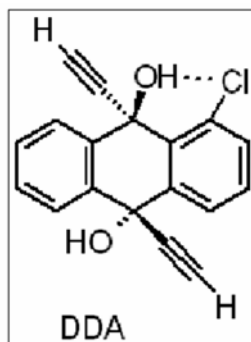


**Figure 2.** Intramolecular O–H...Cl interaction in 1-chloro derivative of trans-9,10-diethynyl-9,10-dihydroanthracene-9,10-diol (DDA). The persistence of this intramolecular geometry in five chloro derivatives was confirmed by X-ray diffraction, <sup>1</sup>H NMR spectroscopy and D<sub>2</sub>O exchange experiments.

directed self-assembly. From the very strong negatively-charged hydrogen bonds and metal–heteroatom coordination bonds to strong and weak hydrogen bonds and interheteroatom interactions span an energy range of 50 kcal/mol (table 1).<sup>7</sup> The esoteric organic chlorine group was examined as an acceptor for OH and CH donors by a few groups. Intramolecular O–H...Cl hydrogen bond in 1-chloro derivatives of trans-9,10-diethynyl-9,10-dihydroanthracene-9,10-diols (DDA, figure 2) was confirmed by NMR spectroscopy and X-ray diffrac-

tion.<sup>8</sup> The intramolecular O–H...Cl hydrogen bond ( $d = 2.25\text{--}2.40 \text{ \AA}$ ) persisted in five out of six structures with varying number of Cl groups on the aromatic core. Of the two OH groups, the free OH resonates at  $\delta$  2.8 ppm in the NMR spectrum whereas the hydrogen bonded OH is significantly downfield at 4.4–4.6 ppm. Moreover, the free OH exchanged with D<sub>2</sub>O immediately but the bonded OH is fully exchanged after 1 h. O–H...Cl hydrogen bond energy of 4.0 kcal mol<sup>-1</sup> (DFT, GAMESS, B3LYP/6 ± 31G\*) is at the upper limit of weak hydrogen bond range (0.5–4.0 kcal mol<sup>-1</sup>). Interactions to the electronegative Cl acceptor are activated by metal and anion nature (Cl–M, Cl<sup>-</sup>) compared to organic chlorine (Cl–C). Coordination compounds of Co, Cu and Zn with bi/tridentate pyrazolyl/pyridyl ligands showed a new C–H...Cl–M inorganic supramolecular synthon.<sup>9</sup> An electron-rich Cl can act as an acceptor from one, two and up to three CH aromatic/methyl donors (mono, di and trifurcation) in C–H...Cl–M hydrogen bonds (2.48–2.88 Å). Involvement of both O–H...Cl and C–H...Cl hydrogen bonds is seen in a hydrate coordination compound. Aromatic  $\pi$ – $\pi$  stacking of pyridyl/pyrazolyl rings gave ladder networks in these crystal structures. An interesting anomaly in O–H...Cl/C–H...Cl interactions compared to O–H...O/C–H...O hydrogen bonds is that, surprisingly, OH donors make longer contacts than CHs, which is quite the opposite with O and N acceptors in hydrogen bonds. Given the

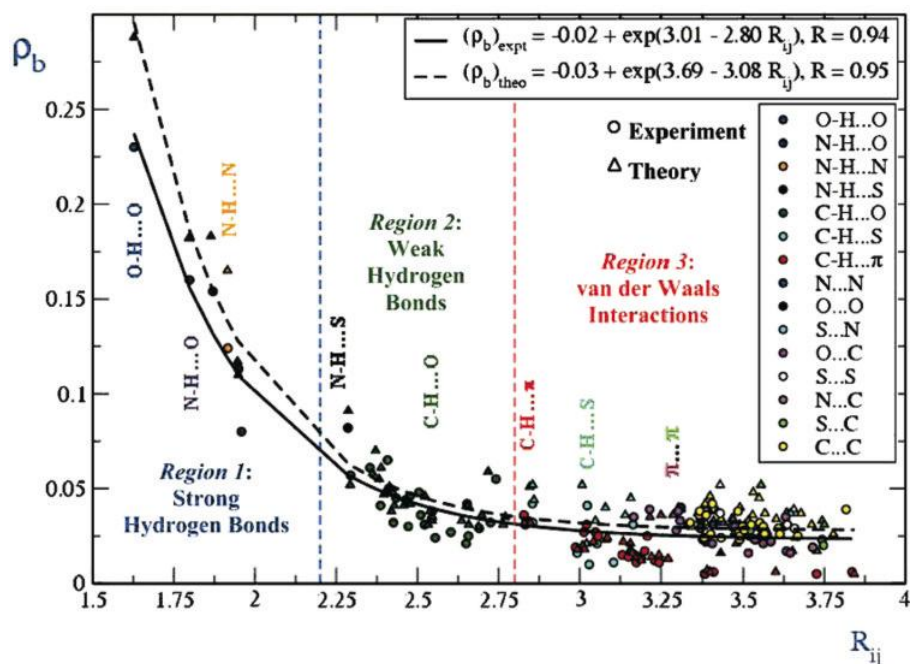


**Figure 3.** Exponential dependence of  $\rho_b$  ( $\text{e}\text{\AA}^{-3}$ ) on  $R_{ij}$  ( $\text{\AA}$ ). Circles and triangles represent experimental and theoretical values and solid and dashed black lines show the corresponding best fit curves. Vertical dashed lines demarcate the three regions of strong H bonds, weak H bonds and van der Waals interactions. See table 1 for energies of these interactions. Reproduced with permission of Royal Society of Chemistry.

bifurcation in these interactions, the term hydrogen bridge<sup>10</sup> was recently resurrected instead of the often used hydrogen bond term.

In a charge density based classification of hydrogen bonds, topological parameters such as electron density ( $\rho_b$ ), Laplacian ( $\nabla^2\rho_r$ ), interpenetration of the van der Waals spheres ( $\Delta r_D + \Delta r_A$ ) correlate well with the length of the interaction line  $R_{ij}$ . Based on  $R_{ij}$  (1.6–3.8 Å) and  $\rho_r$  (0.3–0.005  $\text{e}\text{\AA}^{-3}$ ) values, the continuum of HBs to *vdW* interactions was classified into three regions, shown in figure 3.<sup>11</sup> The strong HB Region 1 of O–H...O/N–H...O HBs has  $R_{ij} < 2.2$  Å and  $\rho_b > 0.1$   $\text{e}\text{\AA}^{-3}$ , Region 2 of C–H...O/N–H...S HBs in range of  $2.2 < R_{ij} < 2.8$  Å and  $0.08 > \rho_b > 0.02$   $\text{e}\text{\AA}^{-3}$ , and finally *vdW* region of  $R_{ij} > 2.8$  Å and  $\rho_b < 0.05$   $\text{e}\text{\AA}^{-3}$  containing C–H... $\pi$ ,  $\pi$ ... $\pi$ , etc. interactions. There is an exponential dependence in  $\rho_b$  vs  $R_{ij}$  curve spanning the three regions for all types of hydrogen bonds and intermolecular interactions, and a remarkable correlation between experimental results and theoretical calculations. In a related study on O–H...O hydrogen bonds<sup>12</sup> electron density at the bond critical point  $\rho_b$  is in the range of 0.03–0.4  $\text{e}\text{\AA}^{-3}$  and its Laplacian is 0.7–6.0  $\text{\AA}^{-5}$ . H...O bond CPs lie in the expected

range but the bond paths are often highly curved and displaced away from the HB axis, by as much as 0.4 Å at the critical point. The hydrogen bond charge density distribution is related not only to the cores of the donor and acceptor atoms but also to the lone pairs as well.

Very short hydrogen bonds are important in enzyme catalysis, proton transfer, drug–receptor recognition and binding, ice structures, and supramolecular chemistry. The traditional view is that short–strong HBs are stabilized by charge or resonance or polarization assistance (CAHB, RAHB, PAHB). Neutron diffraction on a large single crystal of pyrazine-2,3,5,6-tetracarboxylic acid<sup>13</sup> revealed a new type of hydrogen bond shortening phenomenon (H...O 1.5 Å, O...O < 2.5 Å), namely a cooperative, finite array of  $\sigma$ - and  $\pi$ -assistance in the hydrogen bond network. The short O–H...O hydrogen bond (figure 4) of carboxylic acid donor is activated by  $\delta$ -cooperative RAHB and the water acceptor becomes stronger by  $\pi$ -cooperative PAHB in the synthon assisted hydrogen bond (SAHB). That there is no disorder in the H atom position of short O–H...O bond was confirmed in the neutron diffraction Fourier map at 20 K.

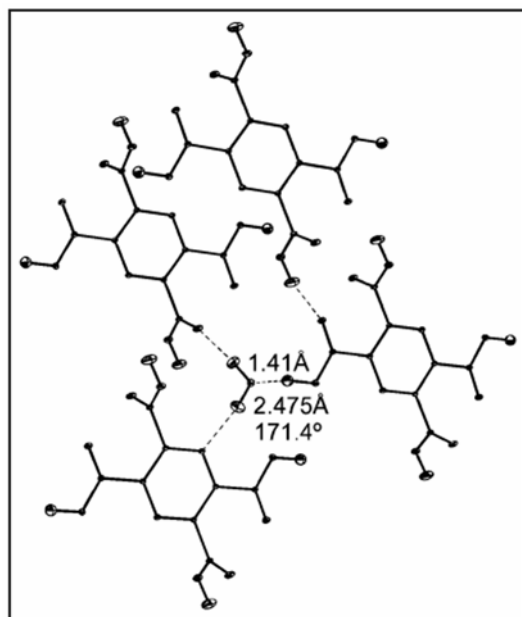


**Figure 4.** Synthon assisted hydrogen bond (SAHB) shortening ( $\text{H}\cdots\text{O}$  1.41 Å) through cumulative  $\pi$ - and  $\sigma$ -cooperative hydrogen bond array in the neutron diffraction crystal structure of 2,3,5,6-pyrazinetetracarboxylic acid at 20 K. Nuclear density is localized on the H atom and there is no evidence of disorder in the calculated Fourier map ( $F_{\text{obs}}$ ). Reproduced with permission of American Chemical Society.

## 2.2 Crystal engineering

Desiraju<sup>6</sup> defined crystal engineering as ‘the understanding of intermolecular interactions in the context of crystal packing and the utilization of such interactions in the design of new solids with desired physical and chemical properties’. The subject was brought into the mainstream of organic chemistry through the concept of supramolecular synthons,<sup>14</sup> which are repeating structural units in crystal structures that are able to guide the rational design of supramolecular architectures based on a small number of recurring hydrogen bond patterns. Whitesides<sup>15</sup> gave a physical organic chemistry interpretation to crystal engineering as ‘the study of molecular and crystal structure correlation in a family of compounds’. A seminal study on hydrogen bonding and crystal packing in amino-phenols highlights the importance of systematic molecular variation to understand crystal structure packing types. In a series of homologous amino-phenol crystal structures, odd and even methylene chain linkers ( $n = 1-5$ ) and  $\text{CH}_2 \rightarrow \text{S}$  isosteric replacement were examined.<sup>16</sup> The expected  $\beta$ -arsenic sheet motif of  $\text{N}-\text{H}\cdots\text{O}$  and  $\text{O}-\text{H}\cdots\text{N}$  hydrogen bonds is the dominant

motif along with square and infinite chain (figure 5) and even  $\text{N}-\text{H}\cdots\pi$  interaction. The even linker structures invariably contained the stable  $\beta$ -As motif whereas the odd series tends towards the sheet motif only when the linker length is long. There is an excellent structural similarity in 4-aminophenol, 4,4'-aminobiphenylol, and the even linker compounds, with all of them containing the  $\beta$ -As sheet but with subtle differences in terms of space group and the network being diamondoid or wurtzite-like. On the other hand, the odd series compound ( $n = 1$ ) has the tetramer  $\text{N}(\text{H})\text{O}$  synthon and more significantly an NH donor that does not participate in conventional H bonding but instead makes  $\text{N}-\text{H}\cdots\pi$  interaction with a phenol ring. The approach geometry of the  $\text{N}-\text{H}\cdots\pi$  interaction to the phenyl  $\text{C}=\text{C}$  bond was confirmed by neutron diffraction (2.39 Å, 155.5°). As the methylene linker becomes longer ( $n = 3, 5$ ) the  $\text{N}(\text{H})\text{O}$  motif changes to infinite chain but the weak  $\text{N}-\text{H}\cdots\pi$  persists. A near linear disposition of OH and  $\text{NH}_2$  groups gives the  $\beta$ -As prototype whereas a bent arrangement, either in meta- and ortho-aminophenols or in odd linker amino-biphenylols, gave square or infinite  $\text{N}(\text{H})\text{O}$  together with the unexpected  $\text{N}-\text{H}\cdots\pi$  interaction.

The common carboxylic acid dimer synthon changes to the rare catemer motif when substituted mesitoic acids have halogen atoms in the meta-positions. Thus weak inter-halogen ( $\text{Cl}\cdots\text{Cl}$ ,  $\text{Br}\cdots\text{Br}$ ) and  $\text{C}-\text{H}\cdots\text{X}$  interactions were shown to direct the helical assembly of strong  $\text{O}-\text{H}\cdots\text{O}$  hydrogen bonds<sup>17</sup>. The structure-directing role of halogen-driven interactions was confirmed in the crystal structure of pentamethyl benzoic acid which formed the expected dimer synthon. In substituted diaryl ureas with  $\text{NO}_2$  and halogen groups, the dominant hydrogen bond synthon is not the expected urea  $\alpha$ -network but urea $\cdots$ nitro  $\text{N}-\text{H}\cdots\text{O}$  synthon ( $\text{X} = \text{Cl}$ ,  $\text{Br}$ ,  $\text{CN}$ ,  $\text{H}$ ,  $\text{Me}$ , etc.). The elusive  $\text{N}-\text{H}\cdots\text{O}$  urea tape in this family was directed by the soft and weak  $\text{I}\cdots\text{O}_2\text{N}$  and  $\text{C}-\text{H}\cdots\text{O}_2\text{N}$  interactions.<sup>18</sup> The idea that strong (hard) and weak (soft) interactions bond pairwise leads to synthon control and crystal design in multifunctional molecules.

The structural motif of amides and reverse amides in homolog series showed that the  $\beta$ -sheet prototype is sustained exclusively by  $\text{N}-\text{H}\cdots\text{O}$  hydrogen bonds in aromatic amides such as PhAm. However, introduction of the pyridyl moiety, e.g. as in 3-PyAm and 3-PyRevAm homologue series (figure 6),<sup>19</sup> gave structures with  $\text{N}-\text{H}\cdots\text{O}$  hydrogen bonds and  $\text{C}-\text{H}\cdots\text{N}$  interactions and  $\text{N}-\text{H}\cdots\text{O}$  and  $\text{N}-\text{H}\cdots\text{N}$

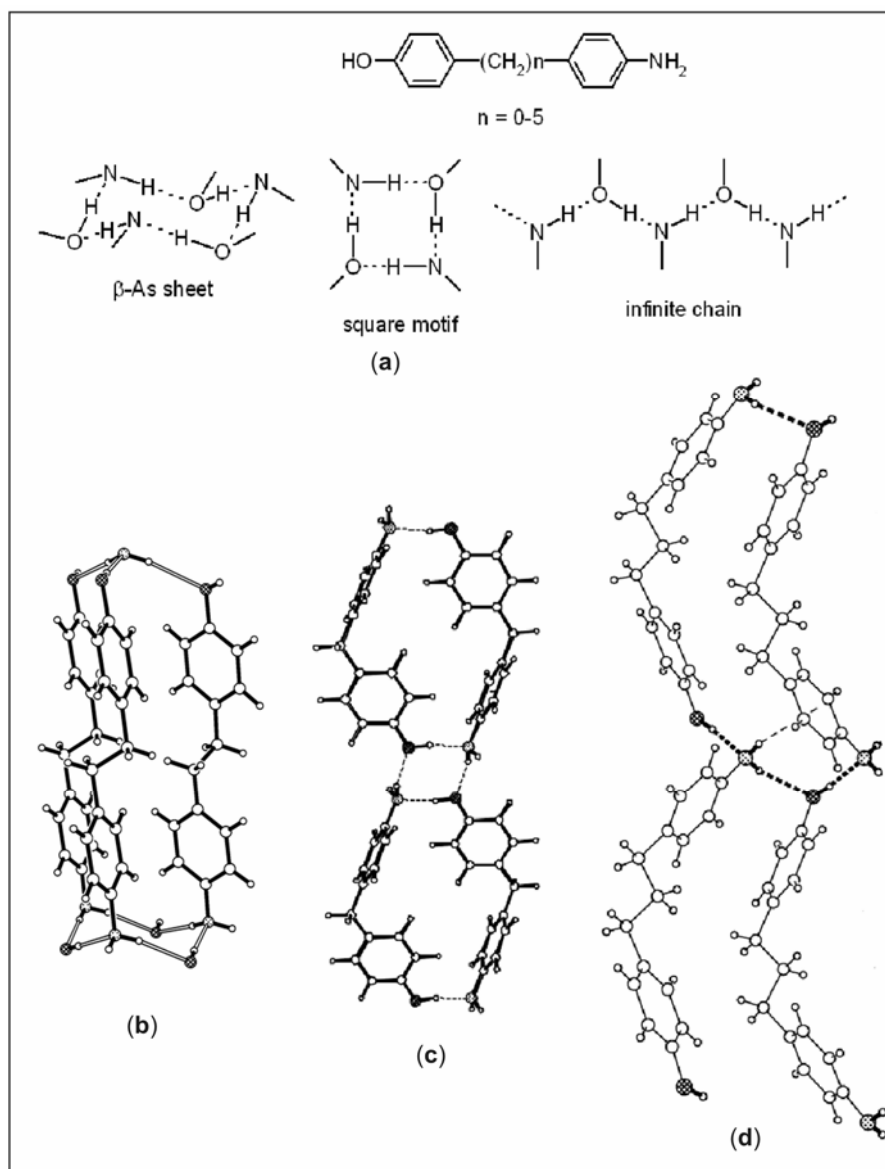


**Figure 5.** (a) Hydrogen bond synthons in homolog series of amino-phenols. (b)  $\beta$ -As sheet in 4-(4-aminophenethyl)phenol ( $n = 2$ ). (c) Square motif in 4-(4-aminophenmethylene)phenol ( $n = 1$ ).  $\text{N}-\text{H}\cdots\pi$  interaction is not seen in this view. (d) Infinite NHO chain in 4-(4-aminophenpropyl)phenol ( $n = 3$ ) and  $\text{N}-\text{H}\cdots\pi$  interaction. Reproduced with permission of American Chemical Society.

hydrogen bonds ( $n = 6$ ), respectively. Thus, while the pyridyl group plays an auxiliary role in 3-PyAm structures it is definitely interfering via  $\text{N}-\text{H}\cdots\text{N}$  hydrogen bond in 3-PyRevAm. 4-PyAm compounds are similar to 3-PyAm but 4-PyRevAm structures crystallized as hydrates. The above examples<sup>17-19</sup> convey that interference from weak halogen or  $\text{C}-\text{H}\cdots\text{O}/\text{N}$  interactions to strong and robust  $\text{O}-\text{H}\cdots\text{O}/\text{N}-\text{H}\cdots\text{O}$  synthons is almost impossible to know prior to X-ray crystal structure analysis. The prediction and control of functional group interfer-

ence, or cross-talk, in hydrogen-bonded structures is a continuing challenge, further complicated by the conformational flexibility of organic molecules.

Carbohydrates are important biomolecules of life. Hydrogen bond patterns in crystal structures of carbohydrates were summarized by Jeffrey and Saenger.<sup>20</sup> (1) maximization of the total number of hydrogen bonds per molecule using as many donor/acceptor oxygen atoms as possible, and (2) maximization of cooperativity by forming as many finite and infinite chains of hydrogen bonds as possible. Inositols and

polyols represent manageable molecular systems to understand the complexities of hydrogen bonding possible in polyhydroxylated molecules. Rigid polyhydroxylated cyclohexanes with *trans* ring fusions (polycyclitols) have 1,3-*syn* OH groups that make an invariant intramolecular O–H...O hydrogen bonded six-member ring (figure 7), and hence the packing of polycyclitols may be understood in terms of a limited number of intermolecular hydrogen bonds with neighbouring molecules.<sup>21</sup> The formation of infinite O–H...O chains is predicted but the number of crystallographic unique molecules (*Z'*) is assumed to be 1 though this is not always the case for diols.<sup>22</sup> In the event, cooperative O–H...O chains and (OH)<sub>4</sub> tetramers of intermolecular hydrogen bonds connect

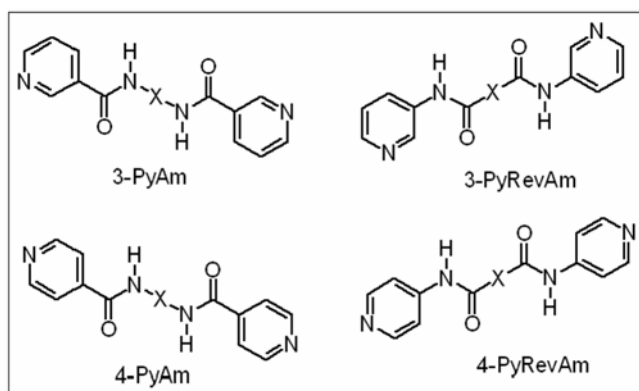


**Figure 6.** 3- and 4-pyridyl amides have a  $\beta$ -sheet or square motif but the reverse amides show very different hydrogen bonding and molecular packing due to perturbation by N–H...N hydrogen bonding and introduction of water in the crystal lattice.

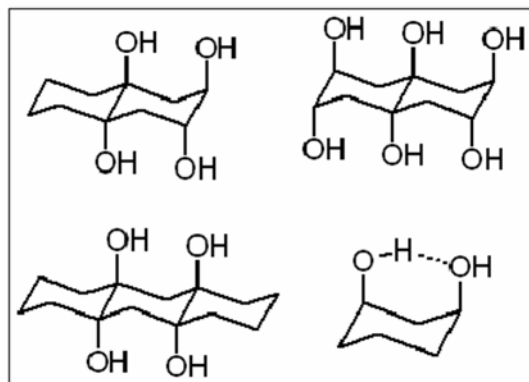


**Figure 7.** Conformationally locked cyclitols with an intramolecular O–H...O hydrogen bond crystallize in a small number of H bonding motifs. Crystal structures of these model compounds help to understand the more complex and unpredictable structures of carbohydrates.

1,3-*syn* diaxial intramolecular H-bonded molecules. By locking the conformational flexibility of the OH group in diaxial orientation through intramolecular H bonds, the packing modes of rigid polyols are predicted in a limited number of hydrogen-bonded architectures.

### 2.3 Supramolecular architectures and network structures

As mentioned in the introduction, host–guest and clathrate structures are the original supramolecular structures, even before the term ‘supramolecular chemistry’ was coined. A supramolecular architecture of alternate open ( $4 \times 4 \text{ \AA}$ ) and closed channels sustained by C–H...O interactions ( $2.4\text{--}2.7 \text{ \AA}$ ) was observed in the cubic symmetry crystal structure of Cu(II) *N*-salicylidene-2-methoxyaniline coordinate complex.<sup>23</sup> The closed channels are filled with phenyl rings of salicylaldehyde. The crystal structure of trigonal molecule *bis*(4-hydroxyphenyl)(phenyl) methane shows symmetry carry-over to supramolecular triangular and hexameric O–H...O synthons in rhombohedral space group  $R\bar{3}$ .<sup>24</sup> Rhombohedral and monoclinic polymorphs of  $\beta$ -hydroquinone were reproduced in phenyl-extended 2,2',6,6'-tetramethyl-4,4'-terphenyldiol,<sup>25</sup> illustrating a fine example of network engineering in polymorphs.

Crystal-to-crystal guest inclusion/release reactions in the solid-state are as such rare. The trinuclear compound  $[\text{Fe}(\mu_3\text{-O})(\mu_2\text{-OAc})_6(2\text{-pyridone})_2(\text{H}_2\text{O})]\text{ClO}_4 \cdot 3\text{H}_2\text{O}$  containing a Fe–OH<sub>2</sub> coordinate bond transformed to Fe–O(H)Me in  $[\text{Fe}(\mu_3\text{-O})(\mu_2\text{-AOc})_6(2\text{-pyridone})_2(\text{MeOH})]\text{ClO}_4 \cdot 3\text{H}_2\text{O}$  while still retaining lattice water and single crystallinity.<sup>26</sup> The methanolyated complex could be regenerated to the hydrate by exposure to atmospheric water vapour without colour loss or X-ray diffraction intensity in a reversible transformation. The reversibility of states was confirmed by IR on MeOH and MeOD complexes. A double [2 + 2] photocyclo addition of alkenes to cyclobutanes was templated by phloroglucinol in the crystalline environment of cocrystal.<sup>27</sup> Reaction of *bis*(pyridinecarboxamido)alkanes with Cu(II) resulted in open 1D chains containing solvent and counterion molecules. 2D layers of (4,4) topology having rhomboidal cavities are either filled with counterions or interpenetrated to give close-packed crystal structures. The exchange of  $\text{ClO}_4^-$  with  $\text{PF}_6^-$  anion resulted in the transformation of 1D

chain to 3D interpenetrated network in an irreversible manner.<sup>28</sup>

Apart from coordination polymers, organometallic clusters too can be used to build supramolecular assemblies via a variety of intermolecular interactions and metal coordination bonds. Hexameric organostannanes [*n*-BuSn(O)OC(O)Ar]<sub>6</sub>, popularly called as drums, contain a structurally similar stannoxane unit made up of prismatic Sn<sub>6</sub>O<sub>6</sub> core.<sup>29</sup> Weak C–H...O, C–H... $\pi$  interactions and  $\pi$ -stacking of aromatic substituents direct the final supramolecular architecture of such organotin drums.

The assembly of lattice inclusion hosts or clathrate compounds has advanced rapidly in the last decade. A three component host lattice made up of 1,3*cis*,5*cis*-cyclohexanetricarboxylic acid (H<sub>3</sub>CTA) hydrogen bonded to 4,4'-bipy-eta and 4,4'-bipy-bu (where eta and bu are (CH<sub>2</sub>)<sub>2</sub> and (CH<sub>2</sub>)<sub>4</sub> methylenes separating 4,4'-bipyridine base). A novel feature of self-assembled termolecular organic host container [H<sub>3</sub>CTA-bipy-eta-(bipy-bu)<sub>0.5</sub>] is that bipy-eta in a gauche conformation builds the closed 1D channels with H<sub>3</sub>CTA, while bipy-bu connects them. A variety of aromatic guest molecules occupy the 10 × 12 Å square cavities.<sup>30</sup> A hierarchic self-assembly model of 1D helices to 2D hexagonal sheets is proposed. Starting from 1,2,4,5-benzenetetracarboxylic acid a variety of aza-acceptors such as 1,10- and 1,7-phenanthroline, phenazine, *bis*-pyridines, etc. were cocrystallized to make sheet-like networks. These complexes crystallize in two broad categories—host-guest compounds with aza partner molecules in channels created by the acid host and supramolecular assemblies of infinite molecular tapes.<sup>31</sup> The tetra-acid does not engage in the usual centrosymmetric COOH dimer but instead makes single O–H...O or O–H...O<sup>−</sup> hydrogen bonds. The adventitious inclusion of water invariably promoted the formation of channels to give host-guest complexes. These 2D sheet structures adopt different stacking modes.

Conglomerate crystallization, or the spontaneous assembly of homochiral crystals as opposed to racemates, is as such a rare phenomenon believed to occur in no more than 5–10% cases.<sup>32</sup> Crystallization of phenols, alcohols and diols/polyols is more likely in enantiomorphous space groups such as *P*2<sub>1</sub> and *P*2<sub>1</sub>2<sub>1</sub>2<sub>1</sub> because OH groups often hydrogen bond via screw axis symmetry.<sup>33</sup> An interesting and unusual example of C–H...Cl interaction (2.7 Å) and  $\pi$ -stacking (3.7 Å) mediated chiral crystallization is

the helical channels in coordination polymer [(L)Zn<sup>II</sup>Cl<sub>2</sub>] (L =  $\alpha,\alpha'$ -*bis*(pyrazolyl)-*m*-xylene). Both left- and right-handed helical polymer chains along the *b*-axis (space group (*P*2<sub>1</sub>) in different crystals from the same batch were identified.<sup>34</sup> Optical rotation of the bulk solution made up of equal amounts of *M* and *P* crystals is zero.

Hydrothermal synthesis of zinc phosphate framework structures starting from amine, phosphoric acid and Zn<sup>II</sup> in suitable solvents gave a variety of supramolecular architectures. Rao and Natarajan<sup>35,36</sup> demonstrated that self-assembly progresses in a hierarchical manner following the Aufbau principle – from 1D chains and ladders to 2D sheets and finally to the 3D frameworks. For example, 1,3-diaminopropane phosphate (DAPP) on reaction with Zn<sup>2+</sup> ions gives a ladder phosphate, [C<sub>3</sub>N<sub>2</sub>H<sub>12</sub>][Zn(HPO<sub>4</sub>)<sub>2</sub>], comprising edge-shared four-membered rings whereas prolonged reaction at 30–50°C yielded a layered structure, [C<sub>3</sub>N<sub>2</sub>H<sub>12</sub>][Zn<sub>2</sub>(HPO<sub>4</sub>)<sub>3</sub>]. The layers are formed from a zigzag chain of four-membered rings, constructed from two Zn and P atoms (Zn<sub>2</sub>P<sub>2</sub>O<sub>4</sub> units), that are connected to each other via two PO<sub>4</sub> units, creating a bifurcation within the layer. Reaction of DAPP with Zn<sup>2+</sup> ions in aqueous solution at 30°C for 24 h gives a product whose XRD pattern shows lines due to the ladder structure while the product obtained from reaction at 50°C (24 h) shows a reflection due to ladder and layer structure (*d*002) at 8.5 Å. Transformation to the layer structure probably occurs through the ladder phase. These results are supported by *in situ* <sup>31</sup>P NMR studies carried out at 85°C, which showed the disappearance of the amine phosphate signal followed by the immediate appearance of a signal due to the precursor phase, before the ladder phase is formed. A generalized scheme of structural relationships and dimensionality evolution was proposed (figure 8) in which the four-membered ring appears to be the first unit formed in the process of building of these complex open-framework structures, which initially form a one-dimensional chain or a ladder structure, and then transform to 2D and 3D structures.<sup>35</sup> In effect, the four-membered rings or/and the one-dimensional structures are the synthons of the more complex structures. The formation of six-, eight-, and higher-membered rings, commonly present in the open framework phosphates, may follow from the 0D/1D structures, with the four-membered rings themselves transforming to the higher rings.

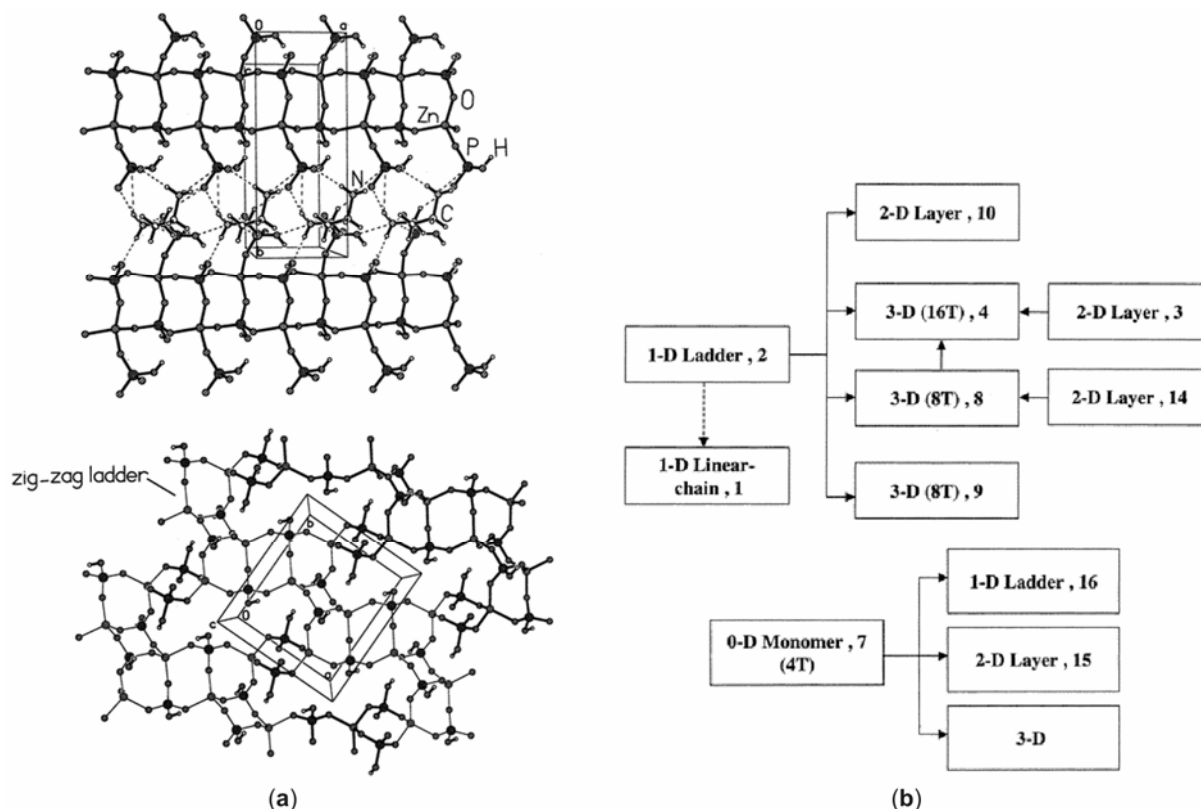


**Figure 8.** (a) 1D ladder phosphate  $[C_3N_2H_{12}][Zn(HPO_4)_2]$  (above) and 2D layer structure of  $[C_3N_2H_{12}][Zn_2(HPO_4)_3]$  (below). (b) Various types of transformations in open framework zinc phosphates. As discussed in the text, features of the 1D ladder phosphate in the 2D layer structure establish an evolutionary relationship in self-assembly. Structural transformations were monitored by XRPD and  $^{31}P$  NMR at different time intervals and temperature ranges. T is tetrahedral framework atom (Zn or P). Refer to original paper<sup>36</sup> for compound numbers. (Reproduced with permission of American Chemical Society).

#### 2.4 Water clusters

*Science* ranked the study of water among the top 10 breakthroughs in 2004.<sup>37</sup> Interest in water clusters of different topologies and dimensionality trapped in small organic and metal-organic crystal structures continued to grow in the current decade. Rare example of planar water hexamers, pentagonal 2D sheets, 1D water helices, and macrocycle water rings were reported by several groups.<sup>38</sup> However, a critical review<sup>39</sup> showed that some of these water motifs were not as remarkable and novel as made out by the original authors. Such an omission in the Google search engine internet age is difficult to condone as mere oversight. Whereas water has a prolific ability to hydrogen bond with polar functional groups and metal centers in a plethora of motifs, the genuine new chemistry generated by water clusters, other than novel structural motifs displayed as colourful images, is an open question.

A solitary exception is crystal structures of sodium saccharinate hydrates.<sup>40</sup> A dihydrate of  $Na_3(sac)_3 \cdot 2H_2O$  (triclinic *PT*, 0.66 water per Na saccharinate) was well-known as the only form whose X-ray coordinates were accurately determined. A monoclinic crystal structure ( $P2_1/n$ ) was solved and refined to good *R*-factor (0.045) for  $Na_{16}(sac)_{16} \cdot 30H_2O$ , which is equivalent to  $Na(sac) \cdot 1.875H_2O$ . This novel hydrate of  $Na(sac)$  has a large unit cell of 15, 614 Å<sup>3</sup> containing 362 atoms (238 non H atoms) in the asymmetric unit.<sup>41</sup> The 64  $Na^+$  cations, 64  $sac^-$  anions, and 120 water molecules in the unit cell make this crystal structure one of the largest and most complex ever for simple ions/molecules. The crystal structure (figure 9) has 'regular' and 'irregular' regions showing certain similarities and differences. In the regular domain, saccharinate anions are nearly parallel and stacked,  $Na^+$  ions are hexacoordinated with water and  $sac^-$ , and water molecules are hydrogen bonded. In the irregular region, there is

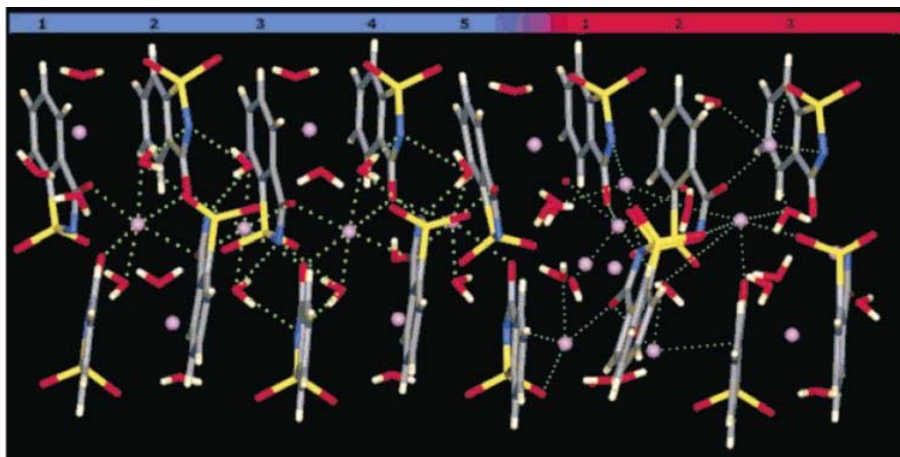


**Figure 9.** Crystal structure of  $\text{Na}(\text{sac}) \cdot 1.875\text{H}_2\text{O}$  (Na pink, O red, N blue, S yellow, C gray, H cream). The regular region on the left side has 10  $\text{sac}^-$  residues and the irregular region on the right has six  $\text{sac}^-$  ions. Note the finite supramolecular cube arrangement. Sac residues are numbered. (Reproduced with permission of Wiley-VCH).

disorder of  $\text{sac}^-$ ,  $\text{Na}^+$  (some of which is not necessarily hexacoordinated), and water (some of which is ill-resolved). The regular region of the structure consists of ten  $\text{sac}^-$  anions, which are arranged in a stack of five water-bridged hydrogen-bonded pairs, with an average interplanar distance of 3.69 Å (figure 9, left side). Two water molecules are involved in each saccharinate pair through strong  $\text{O}-\text{H} \cdots \text{N}$  hydrogen bonds (2.85 Å,  $\theta$  165.9°). Cross-linking of the pairs occurs with octahedrally coordinated  $\text{Na}^+$  ions (mean  $\text{Na}^+ \cdots \text{O}$  2.39 Å). The result is a compact, finite arrangement of  $\text{sac}^-$ ,  $\text{Na}^+$ , and water molecules in the form of three supramolecular cubes and two half-cubes. In the irregular region (figure 9, right side), six  $\text{sac}^-$  anions are not parallel and  $\text{Na}^+$  and water are positionally/orientationally disordered. Based on structure determination at four different temperatures (100, 150, 200, and 298 K) it was concluded that the regular part of the structure resembles a conventional crystal whereas the adjacent irregular region has solution-like characteristics. In effect, the structure represents a state of ‘incipient crystallization’ somewhere between the anhydrate, dihydrate and water rich forms. Most remarkably, and as a very rare case, it was shown that this  $\text{Na}(\text{sac})$  1.875 hydrate crystal picks up and loses water equally easily. Another structural report on saccharinate hydrate appeared simultaneously.<sup>42</sup>

## 2.5 Polymorphism

Research papers on polymorphism dominated the crystal engineering literature in the current decade.

The number of organic polymorphic sets has risen 10 fold, from about 160 in 1995 to >1600 in 2007 (table 2).<sup>43</sup> The record for maximum number of solved crystal structures for the same chemical compound are the seven polymorphs of 5-methyl-2-[(2-nitrophenyl)amino]-3-thiophenecarbonitrile, or ROY, so named because of its red, orange and yellow crystal colours arising from different molecular conformations in different structures. Dimorphs of diphenyl ether (m.p. 20°C) were crystallized by *in situ* cryo-crystallization in a sealed capillary tube at 260–255 K to give a crystal which solved in centrosymmetric space group  $P2_1/n$ . Lowering of the temperature to 240 K and annealing, to improve crystal quality, indeed gave a better quality crystal but in non-centrosymmetric space group  $P2_12_12_1$ .<sup>44</sup> An intramolecular  $\text{C}-\text{H} \cdots \pi$  interaction locks the molecular conformation in both forms. The crystal structure of form I is mediated by a three-dimensional network of  $\text{C}-\text{H} \cdots \pi$  interactions whereas form II has a tetramer of the same interactions. An additional  $\text{C}-\text{H} \cdots \text{O}$  interaction in the latter modification is believed to provide the extra stability to the thermodynamic polymorph II. Subsequent to the isolation of the stable orthorhombic polymorph, the monoclinic form became a disappeared species. Such anecdotes are known for polymorphs.

Polymorphism has important implications in pharmaceutical solid-state formulation, dissolution profile, drug life-cycle management, and tableting. Polymorphism became a major issue in the pharmaceutical industry in the mid-to-late 1990s because of litigation surrounding forms 1 and 2 of Zantac

(Glaxo vs Novpharm) and the accidental appearance of a stable, less soluble form 2 of Ritonavir (Abbott) in production batches. A second polymorph of the popular analgesic aspirin was accidentally discovered during cocrystallization<sup>45</sup> and the structural landscape of aspirin polymorphs were revised.<sup>46</sup> Both form 1 (known) and form 2 (new) crystal structures contain the centrosymmetric O–H...O dimer synthon between COOH groups. However, the difference lies in the way in which these acid dimer layers are connected. In form 1, they are connected through C–H...O dimers related by the inversion center whereas in form 2 they form C–H...O catemers between screw axis related molecules. In effect, identical O–H...O layers are displaced with respect to each other in the two structures. In crystal structure prediction of form 2, it was mentioned that this low energy structure has a low shear elastic constant and hence a low energy barrier to transformation.

To estimate the total domain ratio in a given batch of aspirin crystals, a batch scale factor was introduced into the crystallographic refinements, applied only to reflections with odd  $l$ . The refined value of this scale factor gives the relative weights of form 1 and form 2 reciprocal lattices and therefore a direct estimate of the crystal composition. This procedure would be exact for two perfectly ordered domains with a single domain boundary, but becomes progressively approximate for real aspirin crystals since the extent of domain disorder increases. The procedure gives a total composition estimate but no direct information concerning the sizes of form 1 and 2 domains or their distribution within the crystal lattice. On an unsatisfactorily solved crystal of aspirin, such a refinement against form 2 data set gave  $R_1 = 0.054$  and  $wR_2 = 0.132$ ,<sup>46</sup> a significant improvement on the standard refinement to give refined batch scale factor of roughly 75% form 2 domains. In comparison, an earlier data set ( $R_1$

$0.162, wR_2 0.308$ )<sup>45</sup> solved as form 2 was shown to contain an equal proportion of form 1 and 2 domains.

## 2.6 Cocrystals and salts

Cocrystals are a relatively recently studied class of solid-state structures compared to salts which are well known in the pharmaceutical industry. A very early example of a cocrystal is the 1:1 molecular complex between benzoquinone and hydroquinone, named quinhydrone, reported by Wöhler in 1844. It is the first cocrystal structure in the Cambridge Structural Database<sup>47</sup> with reported coordinates for two polymorphic forms, a monoclinic form in space group  $P2_1/c$  (QUIDON02) and a triclinic structure in  $PT$  space group (QUIDON). There is a resurgence of interest in cocrystals in the last decade or so, particularly because recent experiments suggest that they represent new solid state pharmaceutical forms for solving solubility, hydration, stability and even toxicity issues in drugs.<sup>48</sup> If the supramolecular synthon concept<sup>14</sup> provided rational approaches to crystal synthesis, the classification of synthons as homosynthons (those between like functional groups) and heterosynthons (unlike functional groups) made it possible to dissect cocrystals as being built up from molecules containing complementary functional groups. Thanks to the Cambridge Structural Database,<sup>47</sup> which contains over 450,000 crystal structures and user-friendly fragment and motif search protocols, it is possible to estimate the probability of various synthons in the global archive (figure 10). The hierarchy of homo- and heterosynthon probability in turn becomes the guide to systematic cocrystal design and engineering. The higher probability synthons are more reliable and robust in giving the expected hydrogen bond motif in the designed crystal structure. However, the main issue in carboxylic acid and pyridine cocrystals, i.e. whether the product will be neutral or ionic, remains far from solved.

Cocrystallization of nucleobases with aromatic carboxylic acids<sup>49</sup> gave diffraction quality single crystals of adenine • benzoic acid, cytosine • benzoic acid, cytosine • isophthalic acid, and cytosine • phthalic acid. Nucleobase self-recognition is very strong to give hydrogen-bonded dimers, which are in turn connected via the carboxylic acid. In a related study, trimesic and pyromellitic acid were used as cocrystal formers with cytosine. Now the base dimers were disrupted to give carboxylate...

**Table 2.** Number of 'organic' polymorphs with  $\geq 3$  forms in the CSD. The total number of organic polymorph sets in 1995 was 163, and this number rose 10-fold to ca. 1600 in 2007.

	1995	2000	2002	2005	2007
3 forms	13	27	42	102	124
4 forms	3	3	3	14	20
5 forms	0	0	1	1	3
6 forms	0	0	1	1	0
7 forms	0	0	0	0	1

pyridinium hydrogen bonding in both adducts. In the opinion of this author, the first set of crystal structures<sup>49a</sup> were somewhat unsurprising since the main intent of exploiting directed hydrogen bonding to make cocrystals was not achieved, whereas the second study<sup>49b</sup> successfully achieved the target heterosynthon. A main question that remains unanswered is why the mono- and diacid cofomers gave one structure prototype whereas tri- and tetra-acids afforded a different structure type. The fact that  $pK_a$  decreases as successive COOH groups are added (towards more acidic) in the series benzoic, isophthalic, phthalic, trimesic and pyromellitic acid ( $pK_a$  4.17, 3.46, 2.98, 3.12 and 1.92), could be a factor in going from neutral to ionic synthon. This latter point was brought out in a recent pair of studies on carboxylic acid–pyridine cocrystals wherein the presence of phenol OH group gave neutral cocrystals with O–H...N hydrogen bonding whereas when OH and NH<sub>2</sub> groups were both present the ionic N<sup>+</sup>–H...O<sup>-</sup> was consistently found.<sup>50</sup> These studies alert us to the limitations of the  $\Delta pK_a$  rule in predicting the location of proton in acid–base complexes. It is likely that the presence of additional functional groups in the molecule and their location in the supramolecular environment of the crystal structure modifies the acidity and basicity of functional groups compared to native values for the functional groups. In the absence of accurate  $pK_a$  in

the precise molecular and/or supramolecular environment, the  $\Delta pK_a$  rule should be applied with caution to know neutral–salt states.

The discovery of new synthons adds to the crystal engineering ‘building kit’. Carboxamide...carboxylic acid heterosynthon is well-known in the literature but a limitation with this motif is that its probability of occurrence is modest at 50%, i.e. other motifs might occur in competition, notably the parent homodimers. With the idea of optimizing hydrogen bond acceptor strength for the amide functional group, the pyridine N acceptor was oxidized to the N-oxide resulting in a dramatic increase in acceptor strength. ESP charge in isonicotinamide  $N = -43.7 \text{ kcal mol}^{-1}$ , isonicotinamide-*N*-oxide  $O^- = -53.3 \text{ kcal mol}^{-1}$ ) and  $pK_{\text{HB}}$  of pyridine N, amide O and *N*-oxide O- are 1.86, 1.96 and 2.70 (increasing basicity). The occurrence probability of rationally designed carboxamide...pyridine-*N*-oxide heterosynthon is 80% (figure 10) in diverse crystal structures of APIs and co-formers.<sup>51</sup>

## 2.7 Supramolecular materials

Supramolecular chemistry and crystal engineering practised at the Å and nm scale are the meeting point of ‘top down’ chiseling and ‘bottom up’ construction of nanostructures for materials science and technology. Understanding structure–property correlation and finding the optimal material for a particular application is the goal in these studies. Third order ( $\chi^3$ ) nonlinear optical properties of core-modified porphyrins were shown to depend on the structure of the macrocycle, its molecular conformation, the number of  $\pi$ -electrons, and the extent of conjugation.<sup>52</sup> These factors were evaluated by comparing the structures of modified  $34\pi$  octaporphyrins with reference  $26\pi$  hexaporphyrins (figure 11) and their  $\sigma_2$  values measured by the two-photon absorption process (which are a measure of cubic susceptibility coefficient  $\gamma$ ). Regular porphyrins generally have small  $\sigma_2$  (absorption cross section) in the range 1–10 GM (1 GM =  $10^{-50} \text{ cm}^4 \text{ sec photon}^{-1}$ ) in near-IR wavelength and 100–1600GM in Soret band region. High  $\sigma_2$  values are due to extended conjugation, which increase further with electron-donating substituents in the same macrocycle. The  $34\pi$  octaporphyrins adopt a figure eight conformation that enhances electronic interactions between the thio and seleno linkers compared to the planar  $26\pi$  planar hexaporphyrins. Their exceptionally large GM

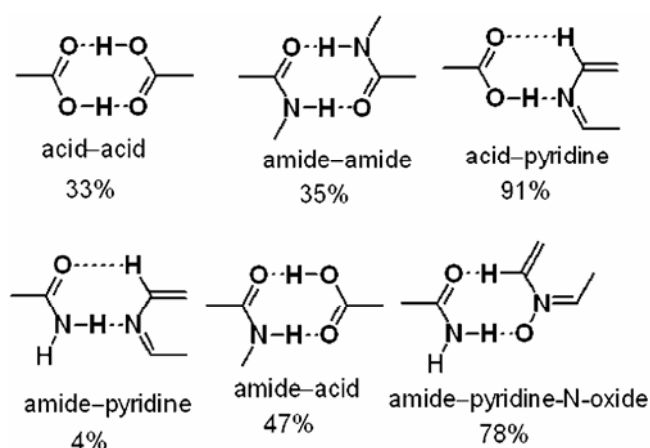


**Figure 10.** Probability of supramolecular homosynthons and heterosynthons in the CSD. The higher the probability of a synthon, the greater is its likelihood of occurrence, or predictability, in crystal structures. A rationally designed novel amide-pyridine-*N*-oxide heterosynthon has high occurrence probability of 80%. In contrast, amide-pyridine synthon having <5% probability has little predictability in cocrystal synthesis.

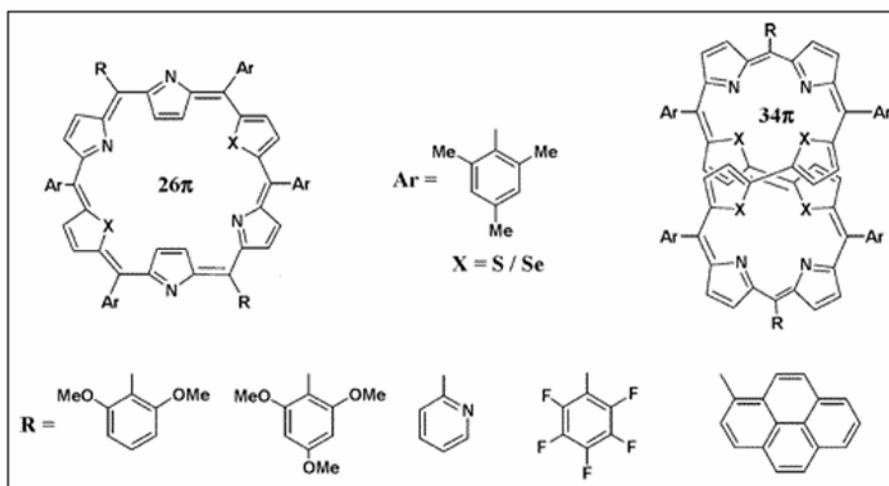


**Figure 11.** Core modified hexaphyrin and octaphyrin analogues for 3rd order NLO materials.  $\sigma_2$  values increase from 2–10,000 GM in  $26\pi$  hexaphyrins to 80–90,000 GM for  $34\pi$  octaphyrins due to enhanced electronic interactions between the inner porphyrin pockets of the ‘figure eight’ macrocycle. Various R groups studied are shown. Reproduced with permission of American Chemical Society.

values (80–90,000 GM) will lead to their applications as organic NLO supramolecular materials whose properties are tunable by rational molecular perturbation.

Polar growth of the non-centrosymmetric polymorph of (4-pyrrolidinopyridyl)*bis*(acetylacetonato) zinc(II) (ZNPPA) in space group *Fdd2* is favoured when the nucleation is done on chiral inorganic surfaces of KDP,  $\text{KBrO}_3$  and  $\text{NaBrO}_3$  to the extent of 27%, 43% and 59%, respectively.<sup>53</sup> On the other hand, there is no preference for chiral crystals compared to solution crystallization upon templating on  $\text{K}_2\text{SO}_4$  and  $\text{Ba}(\text{BrO}_3)_2$  hydrate surfaces. Among  $\text{NaBrO}_3$  crystals of cubic and tetrahedral morphology, the tetrahedral morphology gave higher preferential growth. Most likely, the inorganic template supports heterogeneous nucleation with epitaxial control and oriented growth of ZNPPA crystals.

In order to develop a new family of organogelators, molecular salts of a series of cinnamic acids and *n*-alkyl primary amines were prepared, their X-ray crystal structures analysed, and their gelation behaviour studied.<sup>54</sup> 4-halo-cinnamate salts are gelators and furthermore the chain length of the primary amine has a profound effect on the gelation of 4-Br derivative. The non-gelator salts belonged to space group *PT* whereas the gelators are in *P2<sub>1</sub>/c* crystal setting. All salt structures display an invariant 1D hydrogen bond chain of ammonium...carboxylate bonding. With chain length variation,  $n = 3$ –6 are

non-gelators,  $n = 7$ –15 are gelators and among the latter set  $n = 11$ –15 are better in their gelation property. The gelation behaviour was measured in petrol, kerosene and diesel as test liquids. Alkyl-alkyl interactions in the longer chain gelator salts are responsible for the specific property in this family of salts. However, the 1D fibre in xerogel is different from the single crystal structures as indicated by XRPD patterns.

Fatty acid amide, *n*-lauroyl-L-alanine, is an effective gelator for both aliphatic and aromatic hydrocarbon solvents.<sup>55</sup> Its gelation efficiency increased with the addition of Me groups in the series of solvents benzene, toluene, *p*-xylene and mesitylene. The supramolecular association in the gel is COOH dimer and hydrogen bonding along the  $\text{NHC}=\text{O}$  group such that the alkyl chains adopt a bilayer assembly.

The bile acid template was used for a variety of structural investigations and materials applications such as in molecular recognition, ion receptors/sensors, low molecular mass organo and hydrogelators and gel-nanoparticle composites. Bile acids having  $\pi$ -donor pyrene rings gelled organic solvents in the presence of a  $\pi$ -acceptor fluorenone as a 1 : 1 composite (figure 12).<sup>56</sup> No gelation was observed with either component arguing for a donor-acceptor interaction mediated organogelator. Helical supramolecular architectures through hydrogen bonding and  $\pi$ -stacking interactions are being studied

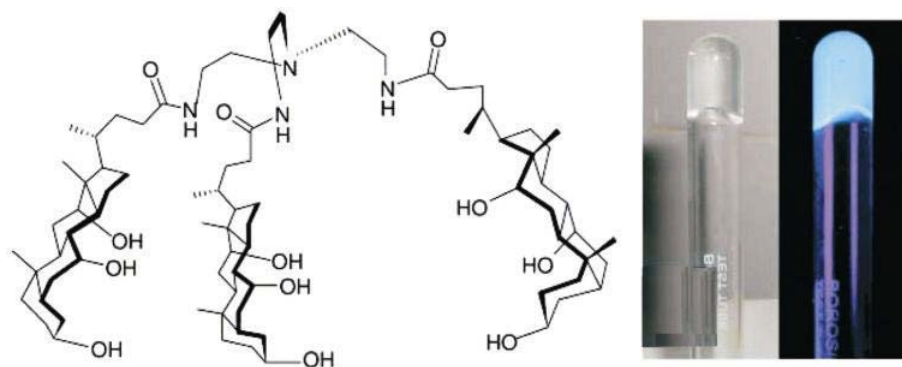


**Figure 12.** Tris cholamide derived hydrogel is colourless but turns blue in long-wave UV light. This luminescent hydrogelator immobilizes water molecules at extremely low 0.15 mM concentration. Reproduced with permission of Royal Society of Chemistry.

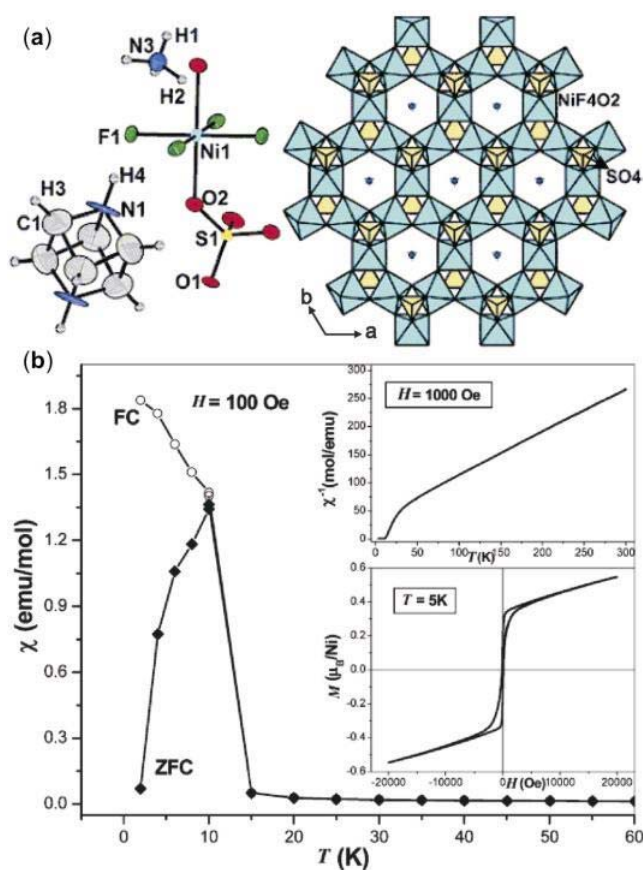


**Figure 13.** (a) Asymmetric unit and hexagonal Kagome layer in  $[\text{C}_6\text{N}_2\text{H}_8][\text{NH}_4]_2[\text{Ni}_3\text{F}_6(\text{SO}_4)_2]$ . (b) Temperature dependence of magnetic susceptibility at 100 Oe under field-cooled (FC) and zero-field-cooled (ZFC) conditions and temperature variation of inverse susceptibility at 1000 Oe were measured (insert). The material shows magnetic hysteresis at 5 K (insert). Reproduced with permission of American Chemical Society.

towards making chiral organogelators. A tripodal derivative functions as a hydrogelator at extremely

low concentration of 0.02% w/v, with one gelator effectively immobilizing  $>10^5$  water molecules.

Transition metal compounds with a Kagome lattice are important because of their magnetic properties. Different metal atoms such as Fe, V, Co, etc. have been studied to give ferromagnetic, antiferromagnetic and ferrimagnetic interactions. Following theoretical models that showed ferro/ferrimagnetic interactions for integral spins and spin frustration for half-integer spins, a  $\text{Ni}^{2+}$  ( $S = 1$ ) Kagome compound (figure 13) having the formula  $[\text{C}_6\text{N}_2\text{H}_8][\text{NH}_4]_2[\text{Ni}_3\text{F}_6(\text{SO}_4)_2]$  was prepared with 1,4-diazacubane ligand.<sup>57</sup> Anionic layers of vertex-sharing  $\text{Ni}^{\text{II}}\text{F}_4\text{O}_2$  octahedra and  $\text{SO}_4$  tetrahedra fused together by Ni–F–Ni and Ni–O–S bonds. The high temperature inverse susceptibility data give a Weiss temperature of 60 K and an effective magnetic moment per nickel atom of  $3.02 \mu_B$ , which is comparable to the value in  $\text{V}^{+3}$  jarosites ( $3.02$ – $3.16 \mu_B$ ). The susceptibility ( $\chi$ ) decreases due to antiferromagnetic superexchange coupling between spin moments ( $S$ ) above 15 K. The coupling is primarily angle-dependent (canted) antiferromagnetic (AFM) induced below 15 K. At even lower temperatures ( $< 10$  K),  $\chi$  decreases due to weak AFM coupling between the layers. The occurrence of such diverse interactions of different magnitudes and signs is due to interplay between the frustrated Kagome geometry and the integer spins of  $\text{Ni}^{2+}$  ions.

The focus so far was on crystalline solids. Compounds that do not crystallize, or amorphous materials, are important in several applications such as soluble drug forms and in optoelectronics. Molecules with rigid structural features find a difficulty in crystallization which at the first level may be reconciled by having multiple molecules in the asym-

metric unit.<sup>22</sup> When this too is difficult, e.g. as in large tetrahedral, spiro fused, star burst and dendrite structures, then the result is amorphous materials. Tetraaryl bimesityls represent such a class of hindered tetrahedral molecules<sup>58</sup> for molecular engineering as amorphous OLED materials (organic light emitting diodes). The UV-Vis absorption of these compounds differs significantly depending on the anthracene substituent groups. Moreover, the molar extinction coefficients ( $\epsilon$ ) of 4-fold functionalized derivatives are almost twice that of 2-fold derivatives (57,200 vs 123,820  $\text{M}^{-1} \text{cm}^{-1}$ ). Photoluminescence spectroscopy studies in dilute solutions ( $\mu\text{M}$  conc.) showed that the emission maxima occur in the blue (430 nm), blue-green (450 nm) and green (485 nm) regions, which were red shifted by 20–50 nm in thin films. Thermal properties indicate

good stability (decomposition temperature  $T_d$  420–520°C) and high glass transition temperatures ( $T_g$  200–300°C). Three types of multilayer devices A, B and C were fabricated. Electroluminescence spectra recorded for the best material showed blue and blue-green emissions (figure 14). Small-molecule-based OLEDs are considered more valuable than polymer counterparts because of difficulty in controlling the film thickness with polymers and the possibility that the first layer may dissolve during spincoating of the second layer. Further, the diversity of organic molecules with varying molecular weights and wide-ranging properties is simply unmatched by inorganic materials.

### 3. Conclusions

#### 3.1 Icons and Holy Grail

The debate on Icons in Chemistry is not new. Many chemists argue that unlike mathematics and physics, chemistry lacks popular statespersons. Tracing the growth of nanotechnology, Philip Ball<sup>59</sup> points out how the origin of this subject goes to Richard Feynman. His famous talk *There's Plenty of Room at the Bottom* on the atom by atom assembly at the American Physical Society meeting in Caltech<sup>60</sup> kick-started the new discipline of nanotechnology exactly fifty years ago (1959). He envisioned back then 'that we could arrange atoms one by one, just as we want them.' Organized assembly of molecules or ions as we know of in Lehn's description of supramolecular chemistry<sup>1,2</sup> is just that. There is a similar chronology to crystal engineering.<sup>6</sup> The chemical leanings of crystal engineering are surely traced to Gerhard Schmidt<sup>5</sup> from his pioneering work on controlled photochemical reactions in the solid-state. The term was, however, first coined by Raymond Pepinsky at the 1955 meeting of the American Physical Society in Mexico City.<sup>61</sup> 'Crystallization of organic ions with metal-containing complex ions of suitable sizes, charges and solubilities results in structures with cells and symmetries determined chiefly by packing of complex ions. These cells and symmetries are to a good extent controllable: hence crystals with advantageous properties can be "engineered".' This definition in effect encompasses the modern scope of crystal engineering as it is practised 50 years later. Even as this article celebrates the contributions of chemists in the last decade covering modern topics of supramolecu-

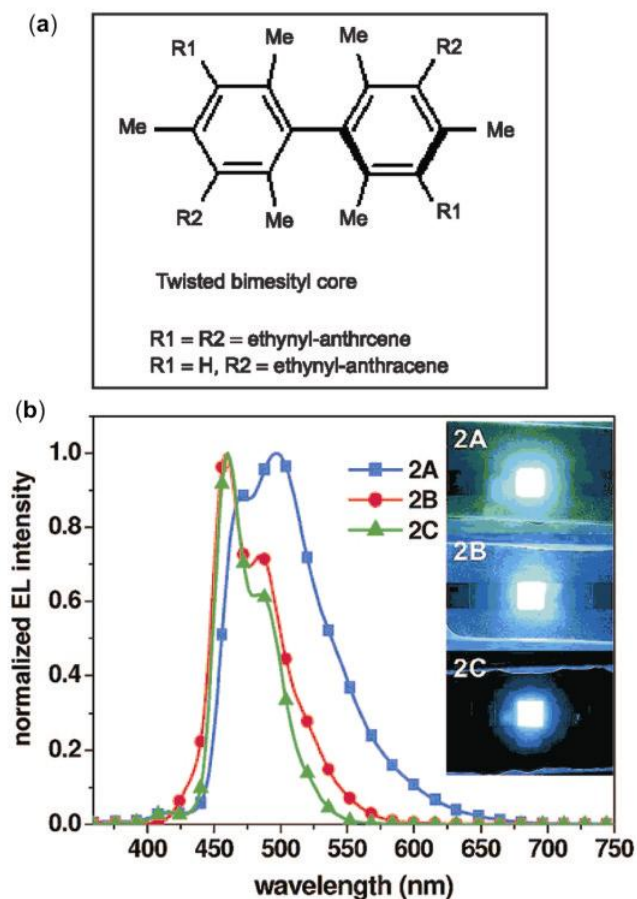


**Figure 14.** (a) Twisted bimesityls of  $D_{2d}$  symmetry synthesized by Sonogashira coupling as amorphous OLED materials. (b) Electroluminescence spectra of the best disubstituted bimesityl compound recorded for three types of multilayer devices, A, B and C are blue-green to blue emitters. Reproduced with permission of American Chemical Society.

lar chemistry, crystal engineering, and nanoscience and nanotechnology, the blueprint of these disciplines were outlined by physicists in the 1950s. Does this mean that chemists must learn to start thinking on a Grand Scale into the Future?<sup>62</sup> A related issue that in part answers why chemists often think and work on multiple problems and not a single Holy Grail<sup>63</sup> is perhaps to do with the very nature of the subject.<sup>64</sup> According to George Whitesides, 'I don't think there is a single thing that would turn all of chemistry on its ear, since one of chemistry's strengths is its diversity.'<sup>65</sup>

### 3.2 Looking forward

It should be clear to the reader that both supramolecular chemistry and crystal engineering are interdisciplinary subjects that define a meeting point for organic, inorganic, physical, and computational chemists along with biologists and materials scientists. The last two decades were the heydays for seamless sciences. This author was trained for his PhD in natural product synthesis and started thinking in the supramolecular direction inspired by a review entitled 'Organic synthesis – where now?' that appeared in the early days of his independent research (1990s).<sup>65</sup> The two facets discussed in this article developed in a time sequence. The nineties saw the rapid emergence of supramolecular chemistry in many fascinating manifestations, described in the *Perspectives in Supramolecular Chemistry* series published from 1994 to 2004.<sup>66</sup> Thanks to the CCD X-ray technology becoming commercial around 1995, the current decade is witnessing a dramatic rise in the spread and popularity of crystal engineering as an independent subject.<sup>67</sup> Given the unique ability of chemists to create their own objects, i.e. molecules, it is certain that chemistry will continue to play a central role in the sciences.

### Acknowledgements

I thank several of my students and coworkers whose names appear in the publications cited in this article. I thank present members of my research group in collating data and references and assistance with graphics during the writing of this article. The Department of Science and Technology, Council of Scientific and Industrial Research, and University Grants Commission are profusely thanked for providing financial assistance and infrastructure facilities.

### References

1. Lehn J-M 1978 *Pure Appl. Chem.* **50** 871–892
2. Lehn J-M 1995 *Supramolecular chemistry: Concepts and perspectives* (Weinheim: VCH)
3. Steed J W and Atwood J L 2000 *Supramolecular chemistry* (Chichester: Wiley)
4. Schalley C A (ed.) 2007 *Analytical methods in supramolecular chemistry* (Weinheim: Wiley-VCH)
5. Schmidt G M J 1971 *Pure Appl. Chem.* **27** 647
6. Desiraju G R 1989 *Crystal engineering: The design of organic solids* (Amsterdam: Elsevier)
7. Desiraju G R and Steiner T 1999 *The weak hydrogen bond in structural chemistry and biology* (Oxford: OUP)
8. Banerjee R, Desiraju G R, Mondal R and Howard J A K 2004 *Chem. Eur. J.* **10** 3373
9. Balamurugan V, Hundal M S and Mukherjee R 2004 *Chem. Eur. J.* **10** 1683
10. Desiraju G R 2002 *Acc. Chem. Res.* **35** 565
11. Munshi P and Guru Row T N 2005 *CrystEngComm* **7** 608
12. Ranganathan A, Kulkarni G U and Rao C N R 2003 *J. Phys. Chem.* **A107** 6073
13. Vishweshwar P, Babu N J, Nangia A, Mason S A, Puschmann H, Mondal R and Howard J A K 2004 *J. Phys. Chem.* **A108** 9406
14. Desiraju G R 1995 *Angew. Chem., Int. Ed. Engl.* **34** 2311
15. (a) Zerkowski J A, Mathias J P and Whitesides G M 1994 *J. Am. Chem. Soc.* **116** 4304; (b) Palacin S, Chin D N, Simanek E E, MacDonald J C, Whitesides G M, McBride M T and Palmore T R 1997 *J. Am. Chem. Soc.* **119** 11807
16. (a) Vangala V R, Bhogala B R, Dey A, Desiraju G R, Broder C K, Smith P S, Mondal R, Howard J A K and Wilson C C 2003 *J. Am. Chem. Soc.* **125** 14495; (b) Dey A, Kirchner M T, Vangala V R, Desiraju G R, Mondal R and Howard J A K 2005 *J. Am. Chem. Soc.* **127** 10545
17. Moorthy J N, Natarajan R, Mal P and Venugopalan P 2002 *J. Am. Chem. Soc.* **124** 6530
18. (a) George S, Nangia A, Lam C-K, Mak T C W and Nicoud J-F 2004 *Chem. Commun.* 1202; (b) Reddy L S, Chandran S K, George S, Babu N J and Nangia A 2007 *Cryst. Growth Des.* **7** 2675
19. (a) Sarkar M and Biradha M 2006 *Cryst. Growth Des.* **6** 202; (b) Rajput L, Singha S and Biradha K 2007 *Cryst. Growth Des.* **7** 2788
20. Jeffrey G A and Saenger W 1991 *Hydrogen bonding in biological structures* (Berlin: Springer-Verlag)
21. Mehta G, Sen S and Ramesh S S 2007 *Eur. J. Org. Chem.* 423
22. (a) Lehmler H-J, Robertson L W, Parkin S and Brock C P 2002 *Acta Crystallogr.* **B58** 140; (b) Brock C P 2002 *Acta Crystallogr.* **B58** 1025
23. Reddy P A N, Nethaji M and Chakravarty A R 2003 *Inorg. Chem. Comm.* **6** 698
24. Sarma R J and Baruah J B 2007 *Cryst. Growth Des.* **7** 989

25. Aitipamula S and Nangia A 2005 *Chem. Commun.* 3159
26. Supriya S and Das S K 2007 *J. Am. Chem. Soc.* **129** 3464
27. Santra R and Biradha K 2008 *CrystEngComm.* **10** 1524
28. Sarkar M and Biradha K 2007 *Cryst. Growth Des.* **7** 1318
29. Chandrasekhar V, Gopal K, Nagendran S, Steiner A and Zacchini S 2006 *Cryst. Growth Des.* **6** 267
30. (a) Bhogala B R, Basavoju S and Nangia A 2005 *Cryst. Growth Des.* **5** 1683; (b) Bhogala B R and Nangia A 2008 *New J. Chem.* **32** 800
31. Arora K K and Pedireddi V R 2003 *J. Org. Chem.* **68** 9177
32. Jacques J, Collet A and Wilen S H 1981 *Enantiomers, racemates and resolution* (New York: Wiley-Interscience)
33. Brock C P and Duncan L L 1994 *Chem. Mater.* **6** 1307
34. Balamurugan V and Mukherjee R 2005 *CrystEngComm.* **7** 337
35. Mandal S and Natarajan S 2002 *Cryst. Growth Des.* **2** 665; (b) Natarajan S, Mandal S, Mahata P, Rao V K, Ramaswamy P, Banerjee A, Paul A K and Ramya K V 2006 *J. Chem. Sci.* **118** 525
36. Rao C N R, Natarajan S, Choudhary A, Neeraj S and Ayi A A 2001 *Acc. Chem. Res.* **34** 80
37. The News Sta. 2004 Splish, splash; *Science* **306** 2013
38. Nangia A 2007 In *Encyclopaedia of supramolecular chemistry* (eds) J L Atwood and J W Steed (New York: Marcel Dekker) **1** 1–9; [www.informaworld.com/10.1081/E-ESMC-1200\\_23838](http://www.informaworld.com/10.1081/E-ESMC-1200_23838)
39. Mascal M, Infantes L and Chisholm J 2006 *Angew. Chem. Int. Ed.* **45** 32
40. (a) Jovanovski G and Kamenar B 1982 *Cryst. Struct. Commun.* **11** 247; (b) Naumov P, Jovanovski G, Abbrecht S and Tergerius L-E 2000 *Thermochim. Acta* **359** 123
41. Banerjee R, Bhatt P M, Kirchner M T and Desiraju G R 2005 *Angew. Chem. Int. Ed.* **44** 2515
42. Naumov P, Jovanovski G, Grupče, Kaitner B, Rae A D and Ng S W 2005 *Angew. Chem. Int. Ed.* **44** 1251
43. Roy S, Banerjee R, Nangia A and Kruger G J 2006 *Chem. Eur. J.* **12** 3777
44. Choudhury A R, Islam K, Kirchner M T, Mehta G and Guru Row T N 2004 *J. Am. Chem. Soc.* **126** 12274
45. Vishweshwar P, McMahon J A, Oliveira M, Peterson M L and Zaworotko M J 2005 *J. Am. Chem. Soc.* **127** 16802
46. Bond A D, Boese R and Desiraju G R 2007 *Angew. Chem. Int. Ed.* **46** 618
47. Cambridge Crystallographic Data Center, [www.ccdc.cam.ac.uk](http://www.ccdc.cam.ac.uk). The current release of the CSD (Ver. 5.30, November 2008, ConQuest 1.11) contains over 450,000 entries
48. (a) Almarsson Ö and Zaworotko M J 2004 *Chem. Commun.* 1889; (b) Aakeröy C B and Salmon D J 2005 *CrystEngComm.* **7** 439; (c) Trask A V and Jones W 2005 *Top. Curr. Chem.* **254** 41; (d) Meanwell N A 2008 *Ann. Rep. Med. Chem.* **43** 373
49. (a) Perumalla S R, Suresh E and Pedireddi V R 2005 *Angew. Chem. Int. Ed.* **44** 7753; (b) Thomas R and Kulkarni G U 2008 *J. Mol. Struct.* **873** 160
50. (a) Sarma B, Nath N K, Bhogala B R and Nangia A 2009 *Cryst. Growth Des.* **9** 1546; (b) Shattock T R, Arora K K, Vishweshwar P and Zaworotko M J 2008 *Cryst. Growth Des.* **8** 4533
51. Babu N J, Reddy L S and Nangia A 2007 Amide–N-oxide heterosynthons and amide dimer homosynthons in cocrystals of carboxamide drugs and pyridine–N-oxides. *Mol. Pharmaceutics* **4** 417–434
52. (a) Rath H, Sankar J, PrabhuRaja V, Chandrashekar T K, Nag A and Goswami D 2005 *J. Am. Chem. Soc.* **127** 11608; (b) Gokulnath S and Chandrashekar T K 2008 *J. Chem. Sci.* **120** 137
53. Prakash M J, Raghavaiah P, Krishna Y S R and Radhakrishnan T P 2008 *Angew. Chem. Int. Ed.* **47** 3969
54. Ballabh A, Trivedi D R and Dastidar P 2006 *Chem. Mater.* **18** 3795
55. Bhattacharya S and Pal A 2008 *J. Phys. Chem.* **B112** 4918
56. (a) Nonappa and Maitra U 2008 *Org. Biomol. Chem.* **6** 657; (b) Mukhopadhyay S, Maitra I, Ira, Krishnamoorthy G, Schmidt J and Talmon Y 2004 *J. Am. Chem. Soc.* **126** 15905
57. Behera J N and Rao C N R 2006 *J. Am. Chem. Soc.* **128** 9334
58. (a) Moorthy J N, Venkatakrishnan P, Natarajan P, Huang D-F and Chow T J 2008 *J. Am. Chem. Soc.* **130** 17320; (b) Moorthy J N, Venkatakrishnan P, Huang D-F and Chow T J 2008 *Chem. Commun.* 2146
59. Ball P 2009 *Chem. World* 58
60. Feynman R 1959 *There's plenty of room at the bottom* (Caltech: American Physical Society) <http://www.its.caltech.edu/~feynman/plenty.html>
61. Pepinsky R 1955 *Phys. Rev.* **100** 971
62. These thoughts came up at an informal discussion of the School of Chemistry faculty with Prof. Goverdhan Mehta, Indian Institute of Science, Bangalore during his visit to University of Hyderabad in January 2009
63. Halford B 2009 *Chem. Engg. News* March 30, 34
64. Desiraju G R 2005 *Curr. Sci.* **88** 374
65. Seebach D 1990 *Angew. Chem. Int. Ed. Engl.* **29** 1320
66. Lehn J-M (Founding ed.) 1994–2004 *Perspectives in supramolecular chemistry*, Vols. 1–8 (Chichester: John Wiley)
67. (a) Tiekink E R T and Vittal J J 2006 *Frontiers in crystal engineering* (Chichester: John Wiley); (b) A second volume is currently in publication and a third volume is being planned for 2010. Private communication, Prof. Edward Tiekink, University of Texas at San Antonio